Pervasive and Mobile Computing 30 (2016) 58–70

Contents lists available at ScienceDirect

Pervasive and Mobile Computing

journal homepage: www.elsevier.com/locate/pmc

Channel measurement-based access point selection in IEEE 802.11 WLANs

Kunho Hong, Jun Pyo Kim, Mun-Suk Kim, SuKyoung Lee *

Yonsei University, Department of Computer Science, 50 Yonsei Ro, Seodaemun-gu, 120-749 Seoul, Republic of Korea

ARTICLE INFO

Article history:
Received 12 April 2015
Received in revised form 28 September 2015
Accepted 17 October 2015
Available online 26 October 2015

Keywords:
AP selection
Throughput prediction
Hidden terminal
Frame aggregation

ABSTRACT

With the wide deployment of IEEE 802.11 Wireless Local Area Networks, it has become common for mobile nodes (MNs) to have multiple access points (APs) to associate with. With the Received Signal Strength Indicator (RSSI)-based AP selection algorithm, which is implemented in most commercial IEEE 802.11 clients, the AP with the best signal strength is selected regardless of the candidate AP's available throughput, resulting in unbalanced distribution of clients among the APs in the network. Several studies have shown performance improvement in not just the new MN (nMN), but also the network as a whole when the selection process considers the current load status of candidate APs. However, the proposed algorithms in these studies assume that there are no hidden terminal problems that severely affect the performance of the network. Hidden terminal problems frequently occur in wireless networks with unlicensed frequencies, like IEEE 802.11 in the 2.4 GHz band. Moreover, none of the previous studies have considered frame aggregation, a major improvement in transmission efficiency introduced and widely deployed with the IEEE 802.11n standard. In this paper, we propose a new AP selection algorithm based on the estimation of available throughput calculated with a model based on the IEEE 802.11 distributed coordination function in consideration of hidden terminal problems and frame aggregation. The proposed algorithm is evaluated through extensive simulation, and the results show that the nMN with the proposed AP selection algorithm can achieve up to 55.84% and 22.31% higher throughput compared to the traditional RSSI-based approach and the selection algorithm solely based on the network load, respectively.

1. Introduction

With the wide deployment of IEEE 802.11 Wireless Local Area Networks (WLANs), it is common for mobile nodes (MNs) like smartphones and laptops to face multiple access points (APs) at the time of connection. Most commercial 802.11 clients scan wireless channels to detect nearby APs and associate with an AP with the strongest Received Signal Strength Indicator (RSSI). Recent studies [1,2] have shown that such RSSI-based selection can cause unbalanced MN distribution on APs across a network. Moreover, this can greatly affect the performance of not only the nMN, but also the already associated MNs.

AP selection is a popular research topic in both academia and industry [1–10], with a goal of providing a network environment with maximum performance and fairness across networks. [3,4] proposed a scheme that collects the ratings of APs from MNs when communicating with APs and makes a selection based on the ratings cached in the MNs. Such ratings-based mechanisms only work when the network status remains similar over time. [5] considers channel condition in the

* Corresponding author.
E-mail address: sklee@yonsei.ac.kr (S. Lee).

http://dx.doi.org/10.1016/j.pmcj.2015.10.018
1574-1192/

selection algorithm and [7–9] sought to predict an AP's load based on the delays between probe request and response transmissions that are used as a metric in their selection algorithm. Unfortunately, [5] and [7–9] analyze neither the network status, such as packet error rate, nor throughput of the network, which lacks precise prediction. [6] proposed a distributed AP selection process using game theory, but under the assumption that all MNs have identical status. The authors of [1,2,10] proposed an algorithm that assumes the available throughput of the candidate APs by dividing the bandwidth by the number of associated MNs; however, this model only considers the saturated condition when all of the MNs in the network transmit continuously. Although [1,10] analytically calculated the packet collision probability in the medium access control (MAC) layer, none of the aforementioned studies provide a numerical analysis of the available throughput of the network. Additionally, none of the studies considered hidden terminal problems that can severely affect not only the nMN's performance, but also the entire network's.

Performance analysis of IEEE 802.11 has also been a popular academic research topic [11–16]; however, no previous studies, to the best our knowledge, proposed a suitable theoretical model to obtain the available throughput for the AP selection mechanism. The authors of [11–15] proposed analytical models to determine network throughput under unsaturated conditions by extending Bianchi's two-dimensional Markov chain modeling of the IEEE 802.11 Distributed Coordination Function (DCF) under saturated conditions [16]. Although the models of the IEEE 802.11 DCF in the aforementioned studies show higher accuracy compared to the methods used in the AP selection algorithms, there are limitations in their direct adoption in the AP selection algorithm. [11] used the temporary variable q to express the degree of load; however, q can only be found if the current status of all of the MNs in the network is known. [12,13] used the packet generation rate of each MN in their analysis models, which is difficult to gather for a joining MN. [14] proposed a model that predicts network throughput based on channel utilization, which is measured by physical carrier sensing and channel monitoring. The model in [14], however, has the same problem of requiring every MN to know all of the others in the network. Also, the hidden terminal problems are not considered in their models. Some studies have taken hidden terminals into account in their models [15,17]; however, they have similar limitations to other studies, as follows. [15] extended [11] to consider the hidden terminal problems in the model, with the requirement of knowing the current status of every MN in the network. [17] proposed an analytical model that considers hidden terminals, but is limited to saturated conditions.

In this paper, we develop a mathematical model of an IEEE 802.11 DCF access scheme that analytically derives the available throughput of a joining MN (i.e., nMN), in both saturated and non-saturated conditions considering hidden terminals from nearby APs as well as the frame aggregation technique by extending the model in [14]. Then, the model that we have proposed provides a distributed algorithm that enables each MN to estimate the maximum available throughput for all candidate APs and to select the AP that can provide the highest throughput. The performance of the proposed algorithm is evaluated through extensive simulation. Results obtained indicate that the mathematical model that we have proposed provides throughput estimation with reasonable computation power, and prove that the throughput of the nMN is based only on channel utilization and average busy duration measured at the MN and a particular AP, regardless of the number of existing MNs connected to the AP.

Our main contributions are as follows:

- To the best of our knowledge, there is no previous proposal that considers contention, hidden terminals and frame aggregation, as we do, in theoretically modeling the available throughput of IEEE 802.11 WLANs.
- The proposed algorithm is designed to be implemented on MNs in a distributed manner so that there is no additional control framework or manager to share the information. In addition, the algorithm requires no complex computation, such as mathematical recursion or multiple integrations.

The remainder of this paper is organized as follows: Section 2 describes the background of this paper. Section 3 presents the mathematical model used to estimate AP throughput and proposes our AP selection algorithm. Sections 4 and 5 present the simulation results and the concluding remarks.

2. Background

The performance of the IEEE 802.11 network has improved with the ratification of new standards. For example, frame aggregation introduced in IEEE 802.11n [18] significantly increases channel utilization efficiency by reducing 802.11 overhead, both physical (PHY) and MAC layers. However, such advances are not considered in most of the AP selection algorithms available both academically and commercially. As well as the advances, wide deployment of the IEEE 802.11 devices increases possibility to interfere with other devices, especially hidden terminals. Hidden terminals in the same or adjacent channels can affect not only the performance of a single MN, but also of the network as a whole; however, they are not considered in most AP selection algorithms as well.

2.1. Frame aggregation

Frame aggregation, which was proposed in [19], improves overall throughput with simple optimization to minimize the non-transmission time. Two types of frame aggregation are defined in the standard [18], the aggregated MAC-level service data unit (A-MSDU) and the aggregated MAC-level protocol data unit (A-MPDU). A-MSDU optimizes the MAC header

by aggregating the frames with the same sender and destination address while each MSDU is separated by the subframe header and padding bits. A-MPDU optimizes the Carrier Sense Multiple Access with Collision Avoidance (CSMA/CA) overhead by aggregating the MPDU separated by the MPDU delimiter and padding bits. The performance improvement with frame aggregation is up to 3-fold with A-MPDU and 4.5-fold with two-level aggregation using both A-MSDU and A-MPDU than without aggregation [20]. However, longer frame size degrades network throughput when a hidden terminal exists [21]. When the frame aggregation technique is used, the effect of hidden terminals should be considered to guarantee higher performance.

2.2. Hidden terminal problem

The hidden terminal problem is common in unmanaged wireless networks such as IEEE 802.11. Communication between two nodes can be interfered with by another node unknown to one of the communication parties, i.e., hidden terminal. Mitigation techniques such as Request-To-Send/Clear-To-Send (RTS/CTS) are adopted in the IEEE 802.11 standard [18] to resolve most of the hidden terminal problems with some cost in performance. However, because of wide deployment of wireless networks at home and at work, hidden terminals also exist, in different but adjacent channels that traditional mitigation techniques cannot resolve. In addition, channel bonding, included in IEEE 802.11ac standard, heralded a whole new era of hidden terminal problems in the 5 GHz network where not all of the channels overlap.

The following assumptions are made throughout this paper.

- No RTS/CTS: In this paper, we only consider the basic access scheme of the CSMA/CA algorithm without the hidden terminal mitigation technique used in the standard (RTS/CTS). Interference from hidden terminal problems in multiple AP conditions, on which our study is focused, can neither be detected nor mitigated by the mitigation technique, since the operating channels of each AP vary. Therefore, the affected MNs cannot acquire the network allocation vector (NAV) duration in RTS/CTS transmissions from MNs in adjacent channels [22,23]. Moreover, physical carrier sensing can reduce the advantage of RTS/CTS since a carrier sensing range (CSR) is longer than RTS coverage [24]. Due to the aforementioned shortcomings, we assume that RTS/CTS is not used in the network.
- No hidden terminals for APs: The antennas on typical APs have higher gains than MNs by over 5 dB. Therefore, APs can cover an MN's detecting area [24]. We assume that APs are not affected by hidden terminal problems and only consider the effects on MNs.

3. Proposed AP selection algorithm

In this section, we describe the proposed AP selection algorithm, which estimates the available throughput of candidate APs and finds the AP that can provide the highest throughput for the nMN. The mathematical analysis of the proposed throughput estimation model and the AP selection algorithm based on the model is described in 3.1 and 3.2 respectively. Table 1 lists the notations and symbols used to describe the proposed algorithm.

3.1. Available throughput estimation

With aggregation the average frame size is longer than without aggregation and the level of aggregation significantly affects the overall performance of the network [18,20]. To estimate the available throughput, we first analyze the frame size and transmission time.

The transmission time of an MSDU, denoted by T_u, is given by

$$T_u = \frac{L_s + L_u + L_b}{R_d}, \tag{1}$$

where L_s, L_u, L_b and R_d are the lengths of a sub-frame header, an MSDU payload, padding bits and the transmission rate of data frames, respectively. The transmission time of an MPDU, denoted by T_p, is given by

$$T_p = \frac{L_d + L_p}{R_p} + \frac{L_m + L_u + L_f + L_b}{R_d} \tag{2}$$

where L_d, L_p, L_m, L_f and R_p are the lengths of a delimiter, a PHY header, a MAC header and an FCS and the basic PHY layer transmission rate, respectively. There are two types of aggregation techniques: A-MSDU and A-MPDU. The techniques are typically used together, which is called two-level aggregation.

Let N_a and N_b be the number of aggregated MPDU and MSDU frames in the two-level aggregation (A-MPDU with A-MSDU), respectively. The total number of aggregated frames in a transmission, denoted by N, can be represented as $N = N_a \times N_b$ in the two-level aggregation [18]. Thus, the average transmission time of aggregated frames, denoted by T_d, with the A-MSDU, A-MPDU and two-level aggregation is given by

Table 1
List of notations used to describe the proposed algorithm.

Notations	Comments
$A(i)$	The set of all of the MNs in the MN i's CSR
$B(i)$	The set of all of the adjacent MNs in the MN i's CSR
$H(i)$	The set of all of the hidden MNs in the MN i's CSR
C_i	The number of busy slots of the MN i for the duration of Δt
c_i	The probability of transmission failure caused by packet collisions
γ	The length of collision period
L_b	The length of padding bits
L_d	The length of a delimiter
L_f	The length of an FCS
L_m	The length of a MAC header
L_p	The length of a PHY header
L_s	The length of a sub-frame header
L_u	The length of an MSDU payload
λ	The packet arrival rate
M	Maximum backoff stage
N	The total number of aggregated frames in a transmission
P_e	The probability that no MN in a set X transmits in the considered slot
P_s	The probability that an MN in a set X transmits in the considered slot
P_t	The probability that at least one MN in a set X transmits in the considered slot
p_i	The probability of failed transmission by collision
q_i	The probability of failed transmission by hidden terminals
R_d	The transmission rate of data frames
R_p	The basic PHY layer transmission rate
S	The throughput of a network
S_i	The throughput of the nMN i
T	The average transmission time of busy slots
T_i	The average transmission time of busy slots of the nMN i
T_d	The average transmission time of aggregated frames
T_f	The average duration of failed transmissions
T_r	The transmission time for the preamble bits
T_s	The average duration of successful transmissions
T_u	The transmission time of an MSDU
T_p	The transmission time of an MPDU
$T_{\Delta t}$	The average transmission time of the nMN i for the duration of Δt
$T_{A(i)}$	The average transmission time of all the MNs in set $A(i)$
$T_{B(i)}$	The average transmission time of all the MNs in set $B(i)$
$T_{H(i)}$	The average transmission time of all the MNs in set $H(i)$
τ_i	The slot access probability of the MN i
$\tau_j^{(i)}$	The slot access probability of the MN j measured at the location of the adjacent MN i
$U_{A(i)}$	The average channel utilization of MNs in set $A(i)$
$U_{B(i)}$	The average channel utilization of MNs in set $B(i)$
$U_{H(i)}$	The average channel utilization of MNs in set $H(i)$
U_i	The average channel utilization of the MN i
W_0	Initial windows size (CWmin)

$$T_d = \begin{cases} T_r + \dfrac{L_p}{R_p} + N \times T_u + \dfrac{L_f}{R_d} & \text{A-MSDU} \\ T_r + N \times T_p & \text{A-MPDU} \\ T_r + N_a \times \left(\dfrac{L_p}{R_p} + N_b \times T_u + \dfrac{L_f}{R_d} \right) & \text{Two-Level} \end{cases} \tag{3}$$

where T_r is the transmission time for the preamble bits. Assuming that $N_a \approx \sqrt{N}$, the average transmission time of two-level aggregation in Eq. (3) can be approximated and rewritten as

$$T_d \approx T_r + \sqrt{N} \times \left(\frac{L_p}{R_p} + \frac{L_f}{R_d} \right) + N \times T_u \tag{4}$$

since $N = N_a \times N_b$.

Let T_s and T_f be the average duration of successful and failed transmissions, respectively. T_s and T_f are $T_d + \text{SIFS} + \text{ACK} + \text{DIFS}$ and $T_d + \text{EIFS}$, respectively. T_f can be rewritten as $T_f = T_s + \epsilon$ since $\text{EIFS} \geq \text{ACK} + \text{SIFS} + \text{DIFS}$, where ϵ is a positive value. The average transmission time of busy slots, denoted by T, is bigger than T_s but smaller than T_f. We can obtain T as follows:

$$T = (T_s \times (1 - p_i)) + (T_f \times p_i) \tag{5}$$

where p_i is the probability of failed transmission by collision.

Let τ_i be the slot access probability of an MN i with the corresponding backoff scheme in DCF. From [16], the probability that at least one MN in a set X transmits in the considered slot, no MN in X is transmitting, or an MN in X successfully transmits, as denoted by P_t, P_e and P_s respectively, are given by

$$P_t = 1 - \prod_{i \in X}(1 - \tau_i), \tag{6}$$

$$P_e = 1 - P_t \tag{7}$$

and

$$P_s = \sum_{i \in X} \tau_i \prod_{j \in X, j \neq i} (1 - \tau_j), \tag{8}$$

respectively. The throughput S can be expressed as

$$S = \frac{P_s N L_u}{P_t T + P_e \sigma}, \tag{9}$$

where σ is a slot time, the duration of an empty slot. To obtain S, τ of all of the MNs in the network should be provided, which is not suitable for AP selection where time is constrained and limited.

Probability τ is affected by the transmission of adjacent MNs in the carrier sensing range; thus, it is difficult to estimate. Additionally, obtaining τ of an MN by monitoring the transmissions would provide different results according to the location of the monitoring MN. Since the estimation model seeks to find the maximum throughput of an nMN, we use the nMN's location as the monitoring location. The slot access probability of an MN j, adjacent node to an nMN i, measured at the location of the nMN i and denoted by $\tau_j^{(i)}$, is used. Equally, the probabilities P_t, P_e and P_s of MNs used from here are assumed to be measured at the location of the nMN i.

Unfortunately, $\tau_j^{(i)}$ varies with any slight changes (such as in transmission rate) of the adjacent MNs and the throughput estimation process needs to be repeated with any new $\tau_j^{(i)}$. To mitigate this issue, in this model, we derive the average channel utilization of an MN from $\tau_j^{(i)}$, denoted by U_i, that is not affected by changes of adjacent MNs. U_i can be expressed as

$$U_i = \frac{C_i T_{\Delta t}}{\Delta t}, \tag{10}$$

where C_i and $T_{\Delta t}$ are the number of busy slots and the average transmission time of MN i for the duration of Δt, respectively.

Let $A(i)$ be the set of all of the MNs in MN i's CSR; let $B(i)$ be the set of all of the MNs in $A(i)$, but without MN i itself; and let $H(i)$ be the set of all hidden MNs to MN i. The average busy slot size of the nMN i, set $A(i)$, $B(i)$ and $H(i)$ is T_i, $T_{A(i)}$, $T_{B(i)}$ and $T_{H(i)}$ respectively. The average channel utilization of the set $A(i)$, denoted by $U_{A(i)}$, can be expressed as

$$U_{A(i)} = \frac{\left(1 - \prod_{j \in A(i)} (1 - \tau_j^{(i)})\right) T_i}{P_t T + P_e \sigma}. \tag{11}$$

Also, $U_{B(i)}$ and $U_{H(i)}$ can be expressed by simply replacing the set $A(i)$ in Eq. (11) with $B(i)$ and $H(i)$ respectively. Since $P_t : \tau_j^{(i)} = U_{A(i)} : U_j$, we get $\tau_j^{(i)}$ with Eq. (11) as

$$\begin{aligned} \tau_j^{(i)} &= U_j \frac{(P_t T_{A(i)} + P_e \sigma)}{T_{A(i)}} \\ &= \frac{U_j \sigma}{(1 - U_{A(i)}) T_{A(i)} + U_{A(i)} \sigma}. \end{aligned} \tag{12}$$

Additionally, τ_i can be obtained by substituting U_i for U_j in Eq. (12). In the saturated condition, slot access probability is maximized. From [16], we can obtain the maximum value of τ_i measured at its location as

$$\max(\tau_i) = \frac{2(1 - 2p_i)}{(1 - 2p_i)(W_0 + 1) + p_i W_0 (1 - (2p_i)^M)} \tag{13}$$

where p_i, W_0 and M are the packet error rate of an MN i, initial window size (CWmin) and maximum backoff stage, respectively.

Hidden terminals can severely affect the performance of a network. In this paper, we consider hidden terminals under unsaturated conditions, where the impact of hidden terminals on the nMN's performance is distinct. However, under saturated conditions, the contention level is already at its peak level, so the impact is difficult to distinguish [17]. Assuming that packets from hidden terminals arrive as a Poisson process of rate λ, the inter-arrival times are exponentially distributed and can be expressed as

$$\chi(i, t) = \frac{1}{\lambda_{H(i)}} e^{-t/\lambda_{H(i)}} \tag{14}$$

where $\lambda_{H(i)}$ is the average packet arrival rate of the MNs in set $H(i)$. The collision period, denoted by γ, is $T_i + T_{H(i)}$ because collision could occur during the transmission time of the MN and hidden terminals. The probability of transmission failure caused by hidden terminals and packet collisions, denoted by q_i and c_i, is given by

$$q_i = \int_0^{\gamma} \chi(i,t)dt = 1 - e^{-\gamma/\lambda_{H(i)}} \tag{15}$$

and

$$c_i = 1 - \prod_{j \in B(i)} (1 - \tau_j^{(i)}). \tag{16}$$

The transmission failure probability of MN i by collision, denoted by p_i, is

$$p_i = 1 - (1 - q_i)(1 - c_i). \tag{17}$$

Thus, the throughput of MN i considering hidden terminals, denoted by S_i, is given by

$$S_i = \frac{(1 - p_i)NL_u\tau_i}{T_{A(i)}\left(1 - \prod_{j \in B(i)} (1 - \tau_j^{(i)})\right) + \sigma \prod_{j \in B(i)} (1 - \tau_j^{(i)})} \tag{18}$$

from Eq. (9).

By applying the Taylor series to Eq. (16), we have

$$\begin{aligned} c_i &= 1 - \prod_{j \in B(i)} (1 - \tau_j^{(i)}) \approx \sum_{j \in B(i)} \tau_j^{(i)} \\ &= \sum_{j \in B(i)} \frac{\sigma U_j}{(1 - U_{A(i)})T_{A(i)} + \sigma U_{A(i)}} \\ &= \frac{\sigma U_{B(i)}}{(1 - U_{A(i)})T_{A(i)} + \sigma U_{A(i)}}. \end{aligned} \tag{19}$$

The average channel utilization of $U_{A(i)}$, $U_{B(i)}$ and $U_{H(i)}$, respectively, is derived from the measured channel utilization of $\tilde{U}_{A(i)}$, $\tilde{U}_{B(i)}$ and $\tilde{U}_{H(i)}$. As the average busy slot size varies by MN, we use $T_{A(i)}$ as the basis for aligning the busy slot size. The average channel utilization of adjacent MNs ($U_{B(i)}$) is given by

$$U_{B(i)} = \frac{T_{B(i)}}{T_{A(i)}} \tilde{U}_{B(i)}. \tag{20}$$

U_i and $U_{H(i)}$ can also be derived from $\tilde{U}_i$ and $\tilde{U}_{H(i)}$ by aligning the busy slot size with $T_{A(i)}$ shown in Eq. (20). Eq. (18) can be rewritten as Eq. (21) using Eqs. (12) and (20). Eq. (21) shows that the throughput of MN i after being associated with an AP is represented as

$$S_i = \frac{NL_u\tilde{U}_i}{T_i}(e^{-Y}) \left(1 - \frac{\sigma \tilde{U}_{B(i)} T_{A(i)}}{T_{B(i)}(1 - \tilde{U}_{A(i)})T_{A(i)} + \sigma \tilde{U}_{A(i)}}\right) \tag{21}$$

where $Y = \tilde{U}_{H(i)}(T_i + T_{H(i)} - 2 \times \text{EIFS})/T_{H(i)}$.

3.2. Proposed algorithm

In this section, we propose an AP selection algorithm based on the available throughput estimation model described in the previous section. The algorithm begins with an nMN i scanning and finding candidate APs. The nMN i sends a probe request message to each channel occupied by the APs. The probe request message includes how long the APs should scan for the channel utilization in terms of the number of beacon intervals (i.e., *dot*11*ChannelUtilizationBeaconIntervals*) and the default value in this paper is 1. When receiving the probe request message from the nMN i, the APs measure the channel utilization and the number of frames sent for the given scanning period (i.e., *dot*11*BeaconPeriod* × *dot*11*ChannelUtilizationBeaconIntervals*). The APs send the probe response message with the channel utilization of a given scanning period, denoted by $\tilde{U}_{ap}$, and the number of frames sent during the scanning period back to the nMN i. The average busy slot time of the AP, denoted by T_{ap}, can easily be computed by dividing the $\tilde{U}_{ap}$ by the number of frames sent by the AP. Note that the proposed algorithm requires a minor change in the standard to include the number of frames sent during the given scanning period in the probe response message. After sending a probe request message, the nMN i measures $\tilde{U}_{B(i)}$ and $T_{B(i)}$ in its CSR by monitoring the busy slot time for the same scanning period. When receiving the probe response message from each AP, the nMN i performs the available throughput estimation process as follows:

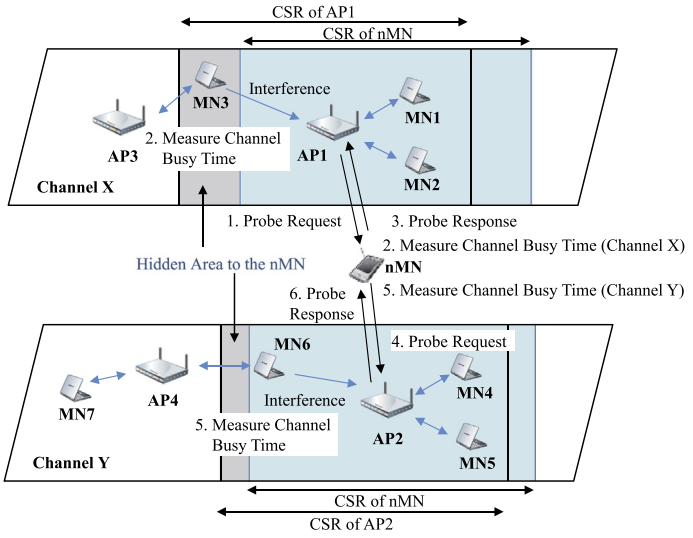

Fig. 1. Working example of the proposed algorithm.

1. Compute $\tilde{U}_{H(i)}$ and $T_{H(i)}$. If $\tilde{U}_{ap} < \tilde{U}_{B(i)}$, $\tilde{U}_{H(i)}$ and $T_{H(i)}$ are zero; otherwise, they are given by

$$\tilde{U}_{H(i)} = \tilde{U}_{ap} - \tilde{U}_{B(i)} \tag{22}$$

and

$$T_{H(i)} = \frac{\tilde{U}_{ap}T_{ap} - \tilde{U}_{B(i)}T_{B(i)}}{\tilde{U}_{ap} - \tilde{U}_{B(i)}}, \tag{23}$$

respectively.
2. Set the data transmission rate (R_D) based on the RSS measured when receiving the probe response message [18], and compute the average transmission time of aggregated frames (T_d) from Eq. (4) by using the values of R_D and the number of aggregated frames (N). Then, compute the average duration of successful (T_s) and failed (T_f) transmissions.
3. Compute the average transmission time of busy slots (T_i) using Eq. (5) where the probability of failed transmission by collision (p_i) is computed from Eqs. (17) and (19).
4. Initialize $\tilde{U}_i$ to 0, and ΔU_i to small value.
5. Increment $\tilde{U}_i$ by ΔU_i.
6. Approximate $\tilde{U}_{A(i)}$ and $T_{A(i)}$. Note that $\tilde{U}_{A(i)}$ is the sum of $\tilde{U}_{B(i)}$ and $\tilde{U}_i$ except the overlapping period. Thus, the $\tilde{U}_{A(i)}$ and $T_{A(i)}$ are approximated as follows:

$$\tilde{U}_{A(i)} = \tilde{U}_i + (1 - p_i)\tilde{U}_{B(i)} \tag{24}$$

and

$$T_{A(i)} = \frac{\tilde{U}_i T_i + (1 - p_i)\tilde{U}_{B(i)}T_{B(i)}}{\tilde{U}_{A(i)}}. \tag{25}$$

7. Compute the average channel utilization (U_i) with the measured channel utilization ($\tilde{U}_i$) using Eq. (20), and calculate the slot access probability (τ_i) by substituting U_i and $\tilde{U}_{A(i)}$ from Eq. (24) for U_j and $U_{A(i)}$, respectively, in Eq. (12).
8. Compute the theoretical maximum value of τ_i in the saturated condition using Eq. (13), and repeat steps 5 to 7 until τ_i in step 7 exceeds the maximum value.
9. Compute S_i using Eq. (21).

The values of p_i and S_i are the expected packet error rate and the estimated throughput of the nMN i when it associates with the candidate AP. With the values, the nMN i selects an AP with the highest S_i among the candidate APs, excluding APs with high packet error rate using the predefined threshold value, p_{th}. Additionally, the minimum throughput requirement can be implemented for vertical hand-over in this algorithm (proposed+). If none of the candidate APs meet the requirement (i.e., all the computed values of S_i are lower than the minimum throughput requirement), the nMN i connects to the cellular network, assuming that the cellular network is available at all times [25].

Fig. 1 illustrates the working example of the proposed AP selection algorithm of an nMN with two candidate APs (AP1 and AP2). AP1 occupies the channel X and AP2 occupies the channel Y. In our algorithm, the nMN sends a probe request to the channel X and measures the channel utilization of the channel X that AP1 occupies. Then, AP1 sends a probe response with

Table 2
Parameters used in simulations.

Parameter	Value	Parameter	Value
R_p	6 Mbps	R_d	54 Mbps
CCA time	4 μs	σ	9 μs
DIFS	34 μs	SIFS	16 μs
CWmin	15	CWmax	1023
Packet size	512 bytes	p_{th}	0.5

the channel utilization and the number of frames sent from the AP. After some computation, as described above, the nMN estimates how much throughput it would get when it associates with the AP. The nMN repeats the process with the channels occupied by other candidate APs (AP2 with the channel Y in this example). Then it connects to an AP that can provide the highest estimated throughput. Note that the estimation and selection process is performed by the MN in a decentralized manner.

For each channel, an nMN sends a probe request message and receives probe response messages from candidate APs occupying the channel. Each response message includes the channel utilization and the number of frames counted from each AP during the scanning period. Around 100 ms (i.e., one beacon period) of scanning time is required per occupied channel [18]. Accordingly, the total time required for the nMN per channel would be around 110 ms considering the scanning time, probe request and response transmissions and transmission delay [26] assuming that there is one candidate AP occupying the channel. Additionally, the most computationally expensive operation in the proposed algorithm is finding the maximum τ_i, which runs in complexity $O(\frac{1}{\Delta U_i})$. We have conducted experiments to measure the run time and found that the available throughput estimation of a candidate AP is completed within 0.1 ms with the Intel Core i7-5500U CPU in low power mode at 900 MHz, when ΔU_i is 0.001. It would take only a few milliseconds with the computational ability of recent smart devices. The overall signaling and computing time per channel is around 115 ms, which is within the limit of the scanning and reassociation time of 2 s of 802.11 devices [27] in the case of a 2.4 GHz spectrum with 11–13 channels or a 5 GHz spectrum with up to 19 channels.

4. Performance evaluation

To evaluate the performance of the proposed algorithm, an IEEE 802.11 MAC simulator is implemented using C++ language. The simulator is based on event-driven architecture with the features including frame aggregation, Clear Channel Assessment (CCA), CSMA/CA and DCF. Packets in the simulator are generated with Poisson distribution. The values of the parameters used to obtain numerical results, for both the analytical model and the simulation runs, are summarized in Table 2.

4.1. Model validation

In this section, we present and discuss the validation of the available throughput estimation model proposed in Section 3.2. The simulation topology has the groups of adjacent (in set $B(i)$) and hidden (in set $H(i)$) MNs to an nMN i. In this scenario, MNs in set $B(i)$ or $H(i)$ constantly transmit packets and the nMN i estimates the available throughput with the proposed estimation model. The numerical analysis is compared with simulation with a varying number of adjacent or hidden MNs of 5, 10 or 20 and a varying number of aggregated frames in nMN's transmission, denoted by N, of 1, 5, 10 and 20. The maximum number of aggregations is set to 20, to limit the maximum aggregated frame size to be 10 kB as in [28]. Also, the difference in performance with the number of aggregated frames more than 20 is minimal when the packet size is 512 kB [29].

Figs. 2 and 3 show the results of the estimation model analysis and the simulations with the different numbers of adjacent and hidden MNs exist and are transmitting. The number of aggregated frames in an nMN i's transmission is set to 10. Fig. 2 represents the throughput estimation of the nMN i in the scenario where only the MNs in set $B(i)$ (i.e., adjacent MNs to the nMN i) are transmitting. The differences between the numerical analysis and the simulation are 1.72%, 1.69% and 1.73% when the number of adjacent MNs is 5, 10 and 20, respectively. Fig. 3 illustrates the scenario when only the MNs in the set $H(i)$ (i.e., hidden MNs to the nMN i) are transmitting. The average difference between the numerical analysis and the simulation is 4.31%, 4.16% and 4.19% when the number of hidden MNs is 5, 10 and 20, respectively. From the results shown in Figs. 2 and 3, we observe that our proposed model can estimate the nMN i's throughput accurately regardless of the number of MNs. We also observe that the increased channel utilization from adjacent MNs degrades the nMN's throughput linearly while the increased channel utilization from hidden terminals degrades the nMN's throughput sharply and exponentially. However, in both cases, the nMN i's throughput is not influenced by the number of contending (adjacent or hidden) MNs. This result is identical to that of Eq. (21) in that there is no relation between the number of contending MNs and the estimated throughput.

We also validated the impact of the number of aggregated frames in an nMN i's transmission in the estimation model. From the discovery that the number of contending MNs has no impact on the proposed model, we set the number of adjacent and hidden MNs to 10 for the rest of the section. Fig. 4(a) and (b) represent the results from numerical analysis and simulation when only MNs in set $B(i)$ (i.e., adjacent MNs to the nMN i) transmit with the number of aggregated frames

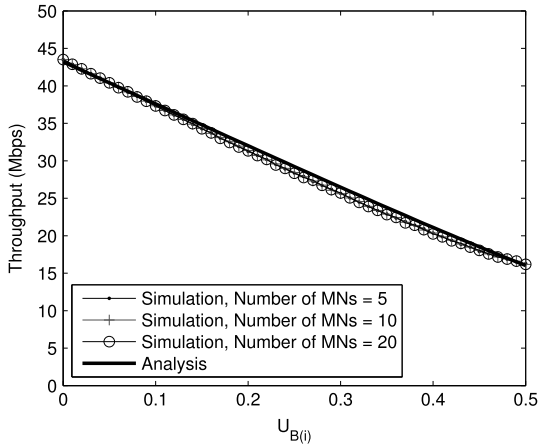

Fig. 2. Estimated throughput of an nMN with only the MNs in set $B(i)$ (i.e., adjacent MNs to the nMN) transmitting: analysis versus simulation with variation in the number of MNs in set $B(i)$ to 5, 10 and 20. The x-axis is the traffic load of MNs in set $B(i)$, varying from 0.0 to 0.5. The y-axis is the estimated throughput.

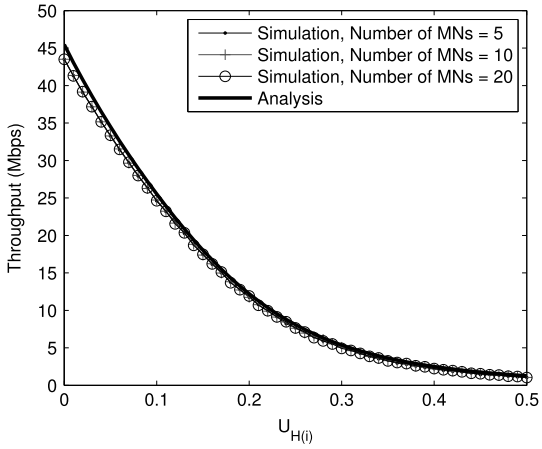

Fig. 3. Estimated throughput of an nMN with only MNs in set $H(i)$ (i.e. hidden MNs to the nMN) transmitting: analysis versus simulation with variation in the number of MNs in set $H(i)$ to 5, 10 and 20. The x-axis is the traffic load of MNs in set $H(i)$, varying from 0.0 to 0.5. The y-axis is the estimated throughput.

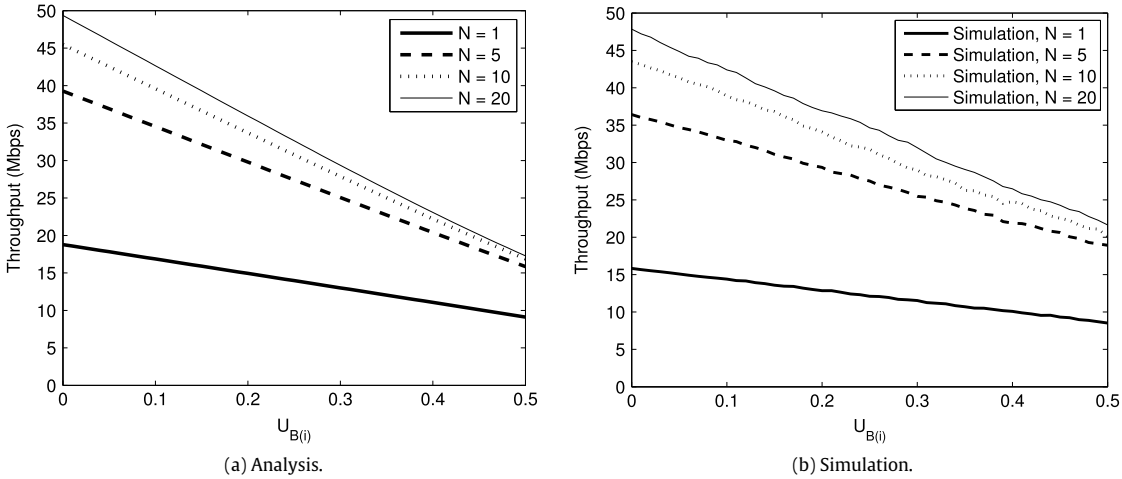

(a) Analysis. (b) Simulation.

Fig. 4. Comparison of an nMN's estimated throughput between analytical results (a) and simulation runs (b) with a varying number of aggregated frames ($N = 1, 5, 10$ and 20) in the nMN's transmission with a fixed number of adjacent MNs (the number of MNs in set $B(i)$ is 10) transmitting. The x-axis shows the traffic load of MNs in set $B(i)$, which varies from 0.0 to 0.5. The y-axis is the estimated throughput.

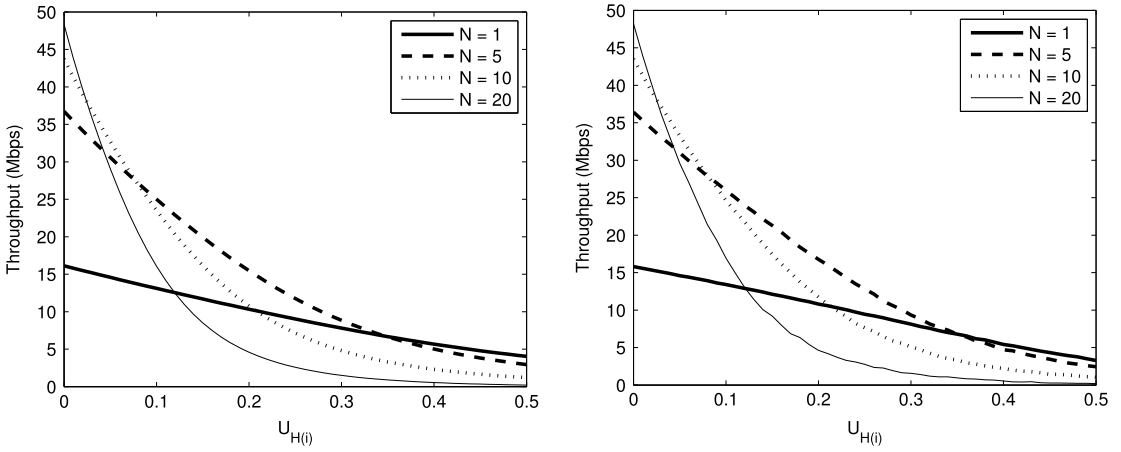

(a) Analysis. (b) Simulation.

Fig. 5. Comparison of an nMN's estimated throughput between analytical results (a) and simulation runs (b) with varying number of aggregated frames ($N = 1, 5, 10$ and 20) in the nMN's transmission with a fixed number of hidden MNs (the number of MNs in set $H(i)$ is 10) transmitting. The x-axis shows the traffic load of MNs in set $H(i)$, which varies from 0.0 to 0.5. The y-axis is the estimated throughput.

in nMN i's transmission varied between 1, 5, 10 and 20. The average throughput from analysis is 11.95, 26.31, 30.83 and 33.70 Mbps and that of the simulation is 12.20, 27.53, 31.72 and 34.51 Mbps when the number of aggregated frames is 1, 5, 10 and 20, respectively. The difference between the analysis and the simulation is 2.09%, 4.64%, 2.89% and 2.40% when the number of aggregated frames is 1, 5, 10 and 20, respectively. The results show that the proposed algorithm estimates nMN i's throughput accurately regardless of the number of aggregated frames in the scenario when only the adjacent MNs are transmitting. We also observe that higher average throughput is achieved with a higher number of aggregated frames in the transmissions.

Fig. 5(a) and (b) represent the results of the numerical analysis and simulation when only MNs in set $H(i)$ (i.e., hidden MNs to the nMN i) are transmitting with the number of aggregated frames in nMN i's transmission varying between 1, 5, 10 and 20. The average throughput of the analysis is 9.38, 14.74, 12.59 and 8.95 Mbps and that of the simulation is 9.17, 15.31, 13.07 and 9.21 Mbps where the number of aggregated frames is 1, 5, 10 and 20, respectively. The average difference between the analysis and the simulation is 2.24%, 3.87%, 3.81% and 2.91% when the number of aggregated frames in nMN i's transmission is 1, 5, 10 and 20, respectively. The results show that the proposed model also estimates the nMN i's throughput accurately, regardless of the number of aggregated frames, in the scenario that only the hidden MNs are transmitting. We have also observed that increased transmission from hidden MNs degrades the throughput of the nMN with a larger number of aggregated frames more drastically. The curves corresponding to $N = 10$ and 20 in Fig. 5 show the exponential decay of the nMN's throughput, as the transmission of hidden MNs increases.

4.2. Simulation result

In this section, we present and discuss the simulation results for the topology in Fig. 6. An indoor space with 4 offices on both sides of the corridor is denoted by A through H clockwise. An AP is located at the center of each office occupying channel X; in addition, four APs in the corridor are marked from 1 through 4 occupying channel Y. Channels X and Y are independent of each other and do not interfere with each other. The indoor path loss model [30] is used in the simulation, with the penetration loss of walls between offices and the corridor being 14 dB and 7 dB, respectively. The transmit power and the minimum received signal sensitivity is set to 0 dBm and −90 dBm, respectively, for each AP to detect MNs and APs in the next and opposite offices. We simulated a scenario with an average of 10 MNs per office by randomly assigning the number of MNs between 0 and 20. The order in which MNs are associated to the APs is chosen randomly in each simulation. Then, each MN checks whether its current AP is still the best at every second. MNs roam from one AP to another if they detect a better one, until the simulation reaches steady state when MNs no longer roam [10]. The results are obtained simulations of 180 s from 120 s to 300 s after the state becomes steady as in [31]. Initially, MNs do not send any transmissions; then, the traffic of each MN increases 100 kbps every second up to 4 Mbps. For the proposed+ algorithm, the minimum throughput requirement is set to 0.5 Mbps. In order to validate the proposed algorithm thoroughly, five different simulations (each with the different number of MNs in the offices) are executed. The results presented in this section represent the average of the five runs. We compare our results using the RSSI-based AP selection and the Online algorithms proposed in [2,5], respectively. A simplified version of the Online algorithm is implemented such that the nMN has all of the required parameters in the network. Note that neither RSSI-based nor Online AP selection algorithms consider hidden terminals in their selection process.

Table 3 describes the results of each selection algorithm in one of the simulation runs. Note that the results from the other runs are similar. The results show that all of the MNs with an RSSI-based AP selection algorithm are connected to the APs in

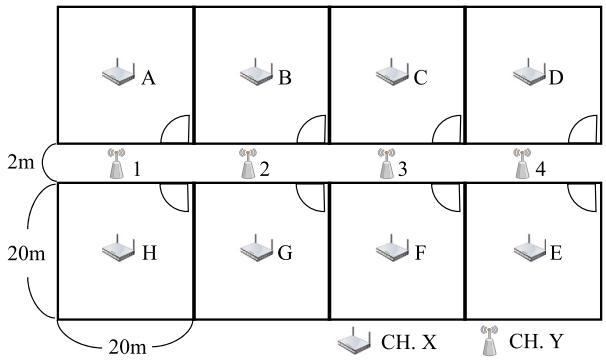

Fig. 6. A typical indoor office WLAN simulation topology.

Table 3
AP selection results for each algorithm.

Algorithms	Selected AP	A (3)[a]	B (17)[a]	C (10)[a]	D (5)[a]	E (3)[a]	F (18)[a]	G (16)[a]	H (8)[a]	Total (80)
RSSI-based	Office	3	17	10	5	3	18	16	8	80
	Corridor	0	0	0	0	0	0	0	0	0
Online	Office	3	11	9	3	3	10	11	4	54
	Corridor	0	6	1	2	0	8	5	4	26
Proposed	Office	3	14	10	5	0	16	0	8	56
	Corridor	0	3	0	0	3	2	16	0	24
Proposed+	Office	0	14	10	5	0	16	0	8	53[b]
	Corridor	0	3	0	0	3	2	16	0	24[b]

[a] Total number of MNs in each office that is randomly selected between 0 and 20.
[b] Three (3.8%) MNs hand-off to the cellular network.

the offices. The MNs with the Online algorithm are connected more to the APs in the offices, with some connected to APs in the corridor. The MNs with the proposed algorithm are connected to APs both in the offices and corridor, since the MNs select an AP with the highest available throughput by considering both the contention level and the channel utilization of each AP. When an MN in an office selects an AP in the corridor, for example, the MN does not experience any throughput degradation in cases without hidden terminals (i.e., no other MNs in different offices select the same AP in the corridor; q_i in Eq. (15) that impacts p_i in Eq. (17) is not increased). However, if some MNs in different offices select and associate with APs in the corridor, they can be potential hidden terminals to MNs in the office that select APs in the corridor in this example. In such cases, the packet error rate (i.e., impacting q_i in Eq. (15)) is increased; this results in performance degradation. Therefore, in this case, selecting the AP in the office would provide higher throughput than selecting one in the corridor. The results show that, with the proposed algorithm, when the MNs in Office B select the AP in the corridor (i.e., AP 2), the MNs in nearby offices select the AP in their offices. Note that all of the MNs in room G are associated with the APs on the corridor not to contend with the MNs in rooms B, H and F that are connected to the APs in the room. Moreover, the MNs in rooms A and C, that can potentially be hidden terminals to the MNs in room G, are not associated with the APs on the corridor; thus, the MNs in room G can utilize the AP in the corridor with less contending (adjacent and hidden) MNs. Lastly, 3.8% of the MNs in the proposed+ algorithm disconnect from APs and connect to the cellular network because of the minimum throughput requirement restriction in the algorithm, decreasing the overall number of MNs to 77 as shown in Table 3. The results from other runs show similar patterns.

Fig. 7(a) demonstrates the aggregated throughput for each algorithm with a varying number of aggregated frames in nMN's transmission of 1, 5, 10 or 20. The aggregated throughput for the RSSI-based, Online, proposed and proposed+ algorithms is 59.14–137.93 Mbps, 82.85–168.47 Mbps, 92.97–198.10 Mbps and 93.59–198.58 Mbps, respectively. Compared with MNs with the RSSI-based algorithm, the aggregated throughput of MNs with the Online, proposed and proposed+ algorithms is increased by 28.39%, 46.85% and 47.26%, respectively. The simulation showed that MNs with the Online algorithm perform with higher throughput than RSSI-based MNs, and with lower throughput than the proposed algorithms. Fig. 7(b) and (c) present the average throughput of the bottom and top 10 MNs during the simulation. The average throughput of the bottom 10 MNs for the RSSI-based, Online, proposed and proposed+ algorithms is 0.20–0.55 Mbps, 0.13–0.23 Mbps, 0.19–0.41 Mbps and 0.79–1.75 Mbps, respectively, and the average throughput of the top 10 MNs for the RSSI-based, Online, proposed and proposed+ algorithms is 1.90–3.61 Mbps, 2.44–3.87 Mbps, 2.51–3.95 Mbps and 2.51–3.96 Mbps, respectively. The top MNs of the Online and proposed algorithms gain 0.38 Mbps and 0.45 Mbps more throughput per MN respectively than the RSSI-based algorithm, with the bottom MNs losing 0.27 Mbps and 0.12 Mbps per MN respectively. The results show that the top MNs with the Online and proposed algorithms perform with higher

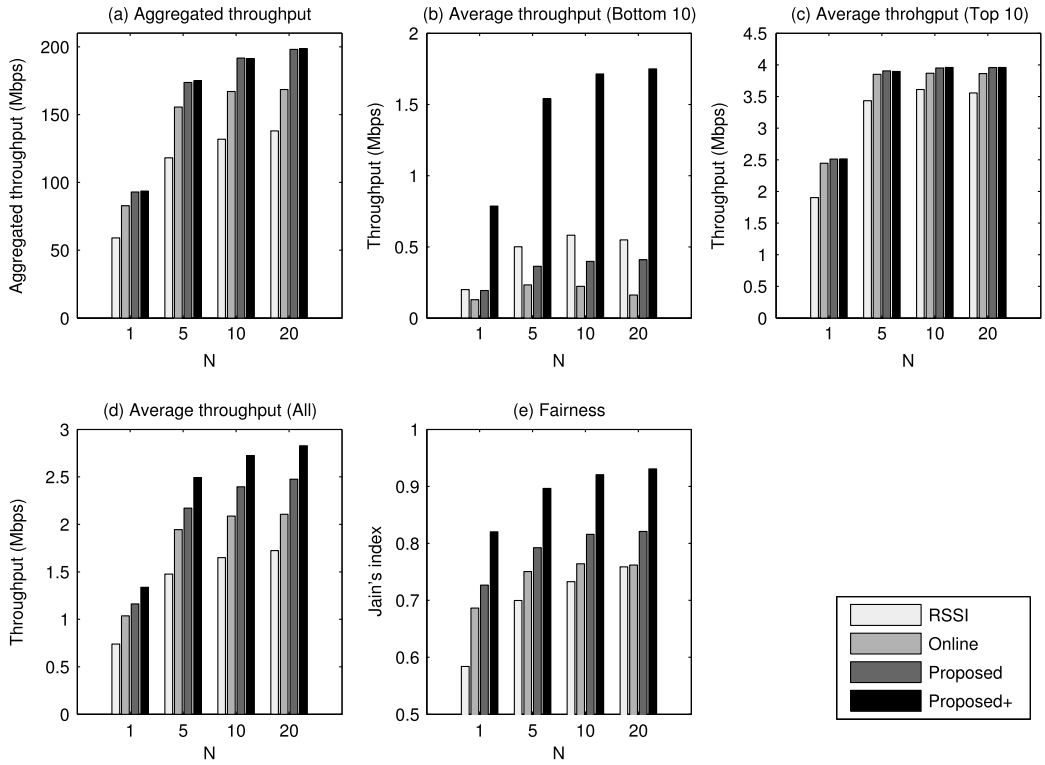

Fig. 7. Simulation results of aggregated throughput for all MNs (a), average throughput of the bottom 10 (b), top 10 (c) and all MNs (d) with the RSSI-based, Online, proposed and proposed+ algorithms with a varying number of aggregated frames in nMN's transmission ($N = 1, 5, 10$ and 20), Jain's Index (e) shows the fairness among the MNs of the algorithms.

throughput than those with the RSSI algorithm, but at the sacrifice of the bottom MNs. However, performance loss of the bottom MNs for the proposed algorithm is only half of that of the Online algorithm, with 18% greater gains. Fig. 7(d) represents the average throughput of all of the MNs in the network for each algorithm. The average throughput of all the MNs with the RSSI-based, Online, proposed and proposed+ algorithms is 0.74–1.72 Mbps, 1.11–2.23 Mbps, 1.16–2.48 Mbps and 1.38–2.83 Mbps, respectively. Jain's Index of each algorithm, representing the fairness between MNs, is 0.694, 0.741, 0.789 and 0.892, respectively, as shown in Fig. 7(e). These results indicate that upon the sacrifice of bottom MNs, the overall performance increases with the proposed algorithm. Note that 3.8% of MNs with the proposed+ algorithm move to the cellular network because the estimated throughput of the MNs is lower than the minimum throughput requirement of the algorithm. The MNs that move to the cellular network are the bottom MNs; therefore, the proposed+ algorithm showed the best performance in terms of the average throughput of the bottom 10 MNs as well as the fairness.

5. Conclusion

There are many unmanaged APs in IEEE 802.11 WLANs. Most of the APs overlap with others, resulting in severe collisions and hidden terminal problems in the network. To select the best AP, we propose an algorithm that estimates the available throughput of accessible APs, considering contention, hidden terminals and frame aggregation. The algorithm predicts network throughput by collecting the channel measurement results of the AP and the nMN; hence, it connects to the AP that can provide the highest throughput. In the simulation, we validated that our proposed algorithm can predict available throughput precisely regardless of the number of contending MNs and aggregated frames. Based on the proposed throughput estimation model, we have also revealed that the aggregated throughput of the network is higher with our AP selection algorithm than with previous models. Through this investigation of a measurement-based AP selection algorithm, we observe that in order to accurately estimate the available throughput an nMN requires to know load information of both sides (candidate AP and the nMN). Moreover, the higher the number of aggregations is, the worse the impact of the hidden terminals is. Lastly, the proposed+ algorithm showed that the proposed algorithm can be applied and extended, with minor modifications, in a vertical hand-over environment, but this needs to be investigated further in future work.

The popularity of channel bonding is growing for IEEE 802.11 WLAN technology [32]. This is related to the occurrence of adjacent channel interference (ACI). Thus, the hidden terminal problem caused by ACI will arise frequently and will degrade performance improvement by channel bonding. Future work should investigate the joint impact of hidden terminals, channel bonding and frame aggregation.

Acknowledgments

This research was supported by the Basic Science Research Program through the National Research Foundation of Korea (NRF) funded by the Ministry of Science, ICT and Future Planning (NRF-2013R1A1A3005914) and the MSIP (Ministry of Science, ICT and Future Planning), Korea, under the ITRC (Information Technology Research Center) support program (IITP-2015-H8501-15-1019) supervised by the IITP (Institute for Information & Communications Technology Promotion).

References

[1] G. Athanasiou, T. Korakis, O. Ercetin, L. Tassiulas, A cross-layer framework for association control in wireless mesh networks, IEEE Trans. Mob. Comput. 8 (1) (2009) 65–80.
[2] F. Xu, X. Zhu, C. Tan, Q. Li, G. Yan, J. Wu, SmartAssoc: Decentralized access point selection algorithm to improve throughput, IEEE Trans. Parallel Distrib. Syst. 24 (12) (2013) 2482–2491.
[3] A.J. Nicholson, Y. Chawathe, M.Y. Chen, B.D. Noble, D. Wetherall, Improved access point selection, in: Proceedings of the 4th International Conference of MobiSys 2006, Uppsala, Sweden, 2006, pp. 233–245.
[4] J. Pang, B. Greenstein, M. Kaminsky, D. McCoy, S. Seshan, WiFi-reports: Improving wireless network selection with collaboration, IEEE Trans. Mob. Comput. 9 (12) (2010) 1713–1731.
[5] H. Wu, K. Tan, Y. Zhang, Q. Zhang, Proactive scan: Fast handoff with smart triggers for 802.11 wireless LAN, in: INFOCOM 2007, May 2007, pp. 749–757.
[6] I. Malanchini, M. Cesana, N. Gatti, Network selection and resource allocation games for wireless access networks, IEEE Trans. Mob. Comput. 12 (12) (2013) 2427–2440.
[7] J.-C. Chen, T.-C. Chen, T. Zhang, E. van den Berg, WLC19-4: Effective AP selection and load balancing in IEEE 802.11 wireless LANs, in: GLOBECOM 2006, November 2006, pp. 1–6.
[8] S. Vasudevan, K. Papagiannaki, C. Diot, J. Kurose, D. Towsley, Facilitating access point selection in IEEE 802.11 wireless networks, in: 5th ACM SIGCOMM Internet Measurement Conference, Berkeley, CA, USA, 2005, pp. 26–26.
[9] I.-P. Hsieh, F.-M. Chang, S.-J. Kao, Adaptive access points selection for 802.11 wireless networks, in: Proceedings of the Fourth IASTED Asian Conference on Communication Systems and Networks, 2007, pp. 218–222.
[10] D. Gong, Y. Yang, AP association in 802.11n WLANs with heterogeneous clients, in: INFOCOM 2012, March 2012, pp. 1440–1448.
[11] D. Malone, K. Duffy, D. Leith, Modeling the 802.11 distributed coordination function in nonsaturated heterogeneous conditions, IEEE/ACM Trans. Netw. 15 (1) (2007) 159–172.
[12] F. Daneshgaran, M. Laddomada, F. Mesiti, M. Mondin, Unsaturated throughput analysis of IEEE 802.11 in presence of non ideal transmission channel and capture effects, IEEE Trans. Wireless Commun. 7 (4) (2008) 1276–1286.
[13] O. Tickoo, B. Sikdar, Modeling queueing and channel access delay in unsaturated IEEE 802.11 random access MAC based wireless networks, IEEE/ACM Trans. Netw. 16 (4) (2008) 878–891.
[14] K. Hong, S. Lee, K. Kim, Y. Kim, Channel condition based contention window adaptation in IEEE 802.11 WLANs, IEEE Trans. Commun. 60 (2) (2012) 469–478.
[15] O. Ekici, A. Yongacoglu, IEEE 802.11a throughput performance with hidden nodes, IEEE Commun. Lett. 12 (6) (2008) 465–467.
[16] G. Bianchi, Performance analysis of the IEEE 802.11 distributed coordination function, IEEE J. Sel. Areas Commun. 18 (3) (2000) 535–547.
[17] B. Jang, M. Sichitiu, IEEE 802.11 saturation throughput analysis in the presence of hidden terminals, IEEE/ACM Trans. Netw. 20 (2) (2012) 557–570.
[18] IEEE Standard 802.11, Wireless LAN Medium Access Control (MAC) and Physical Layer (PHY) specifications, June 2007.
[19] Y. Xiao, IEEE 802.11n: Enhancements for higher throughput in wireless LANs, IEEE Trans. Wireless Commun. 12 (6) (2005) 82–91.
[20] D. Skordoulis, Q. Ni, H.-H. Chen, A. Stephens, C. Liu, A. Jamalipour, IEEE 802.11n MAC frame aggregation mechanisms for next-generation high-throughput WLANs, IEEE Wirel. Commun. Mag. 15 (1) (2008) 40–47.
[21] A. Tsertou, D. Laurenson, Revisiting the hidden terminal problem in a CSMA/CA wireless network, IEEE Trans. Mob. Comput. 7 (7) (2008) 817–831.
[22] V. Angelakis, S. Papadakis, V. Siris, A. Traganitis, Adjacent channel interference in 802.11a is harmful: Testbed validation of a simple quantification model, IEEE Commun. Mag. 49 (3) (2011) 160–166.
[23] J. Nachtigall, A. Zubow, J.-P. Redlich, The impact of adjacent channel interference in multi-radio systems using IEEE 802.11, in: IWCMC 2008, August 2008, pp. 874–881.
[24] K. Xu, M. Gerla, S. Bae, Effectiveness of RTS/CTS handshake in IEEE 802.11 based Ad Hoc networks, Ad Hoc Networks 1 (1) (2003) 107–123.
[25] L.-C. Wang, S. Rangapillai, A survey on green 5G cellular networks, in: IEEE SPCOM 2012, July 2012, pp. 1–5.
[26] D. Murray, M. Dixon, T. Koziniec, Scanning delays in 802.11 networks, in: NGMAST 2007, September 2007, pp. 255–260.
[27] M. Abusubaih, J. Gross, S. Wiethoelter, A. Wolisz, On access point selection in IEEE 802.11 wireless local area networks, in: IEEE Local Computer Networks 2006, November 2006, pp. 879–886.
[28] K.-H. Chou, W. Lin, Performance analysis of packet aggregation for IEEE 802.11 PCF MAC-based wireless networks, IEEE Trans. Wireless Commun. 12 (4) (2013) 1441–1447.
[29] A. Saif, M. Othman, S. Subramaniam, N. Hamid, An enhanced A-MSDU frame aggregation scheme for 802.11n wireless networks, Wirel. Pers. Commun. 66 (4) (2012) 683–706.
[30] Indoor Path Loss, June 2012. [Online]. Available: http://ftp1.digi.com/support/images/XST-AN005a-IndoorPathLoss.pdf.
[31] Y. Fukuda, T. Abe, Y. Oie, Decentralized access point selection architecture for wireless LANs, in: Wireless Telecommunications Symposium, 2004, May 2004, pp. 137–145.
[32] O. Bejarano, E. Knightly, M. Park, IEEE 802.11ac: From channelization to multi-user MIMO, IEEE Commun. Mag. 51 (10) (2013) 84–90.